Aquaculture Research

Aquaculture Research, 2017, **48**, 4420–4428 doi: 10.1111/are.13267

Qualitative analysis of cartilaginous jaw element malformation in cultured yellowtail kingfish (*Seriola lalandi*) larvae

Betzabel Jara[1], Marcelo Abarca[2], Rodolfo Wilson[2], Sebastián Krapivka[3], Ana Mercado[4], Ricardo Guiñez[5] & Lorena Marchant[1,6]

[1]Departamento Biomédico, Facultad de Ciencias de la Salud, Universidad de Antofagasta, Antofagasta, Chile

[2]Departamento de Ciencias Acuáticas y Ambientales, Facultad de Ciencias del Mar y Recursos Biológicos, Universidad de Antofagasta, Antofagasta, Chile

[3]Departamento de Antropología, Facultad de Ciencias Sociales, Universidad de Chile, Santiago, Chile

[4]Departamento de Biotecnología, Facultad de Ciencias del Mar y Recursos Biológicos, Universidad de Antofagasta, Antofagasta, Chile

[5]Instituto de Ciencias Naturales Alexander von Humboldt, Facultad de Ciencias del Mar y Recursos Biológicos, Universidad de Antofagasta, Antofagasta, Chile

[6]Departamento de Ciencias Biológicas y Químicas, Facultad de Ciencia, Universidad San Sebastián, Santiago, Chile

Correspondence: L Marchant, Facultad de Ciencia, Universidad San Sebastián, Lota 2465, Campus Los Leones, Santiago, Chile. E-mail: lore.marchant@gmail.com

Abstract

A central problem facing worldwide culture of yellowtail kingfish (*Seriola lalandi*) is the presence of skeletal malformations, including jaw deformities. This study presents a morphological characterization of normal and abnormal cartilage jaw structures during early larval development. Samples of 70–150 larvae were collected from three cohorts from 2 to 9 days post hatching, anaesthetized and fixed for cartilage staining. Cartilaginous components were defined clearly at four days post hatch (dph) (4.65 ± 0.05 mm total length), and abnormal jaw structures were detectable at this time. Jaw deformities observed included extension of Meckel's cartilage with or without ventral bending of the anterior tip, displacement of ceratohyal and hypohyal cartilage ventrally and below Meckel's cartilage, and shortening and dorsal flexion of the lower jaw. At 4 dph, between 44% and 47% of all larvae examined had jaw abnormalities. The contribution of each deformity to the total number of deformities was variable among the three cohorts examined. To compare shape difference accurately we performed an exploratory, landmark-based geometric morphometric analysis using seven homologous landmarks. Larvae were classified into three jaw morphology groups. The geometric morphometric approach provides a useful tool to standardize classification of cartilage jaw abnormalities at early developmental larval stages. Early recognition of developing abnormalities is of importance for fish farmers in both improving fish selection efficiency and for evaluating effects of rearing parameters.

Keywords: larval development, landmark shape analysis, jaw deformities, *Seriola lalandi*

Introduction

The yellowtail kingfish, *Seriola lalandi* (Perciformes, Carangidae), is a circumglobal species that supports important commercial fisheries in many countries, including Australia, New Zealand and Japan. The species also is used widely in commercial aquaculture because of its fast growth and excellent flesh quality (Poortenaar, Hooker & Sharp 2001; Moran, Smith, Gara & Poortenaar 2007; Moran, Pether & Lee 2009). Because of increasing commercial importance worldwide and occurrence along the Chilean north coast and

Juan Fernández Island, yellowtail kingfish represent an excellent candidate for Chilean aquaculture diversification, currently limited primarily to salmonids (Ibieta, Tapia, Venegas, Hausdorf & Takle 2011). Production of *S. lalandi* in Chile is increasing due to the support of government agencies and programmes for diversification of the Chilean aquaculture industry (PDACH) (Fernández, Cichero, Patel & Martinez 2015), including the pioneer programme initiated by the University of Antofagasta in which hatchery production relies on broodstock derived from locally captured wild fish (Wilson, Ramos, Abarca & Plaza 2012). The improved culture conditions have permitted hatcheries to annually produce larvae and juveniles. However, an unsolved issue affecting quality of hatchery-produced yellowtail juveniles is the high incidence of jaw and operculum deformities affecting 20–70% of juveniles, with considerable variation among batches of eggs. The malformed (abnormal) fish have significantly reduced biological performance in terms of swimming ability and growth rate (R. Wilson, pers. comm.). The only solution currently available to manage this problem is to remove abnormal juveniles manually after 45 dph, at which time deformities can be detected visually. This process is labour intensive, time-consuming and increases production costs.

Jaw malformation in commercially cultured species of *Seriola* is a significant concern in all production hatcheries and in a wide range of other cultured fish species (Cobcroft & Battaglene 2013). Cultured species with jaw abnormalities include European sea bass (*Dicentrarchus labrax*), with twisted and shortened upper and lower jaws (Barahona-Fernandes 1982; Daoulas, Economou & Bantavas 1991); red sea bream (*Pagrus major*), with shortened lower jaw and/or lower and upper jaw (Matsuoka 2003); Atlantic halibut (*Hippoglossus hippoglossus*), with bending of the upper and lower jaws (Lewis & Lall 2006; Cloutier, Lambrey de Souza, Browman & Skiftesvik 2011); striped trumpeter (*Latris lineata*), with open jaws with the maxilla and premaxilla aligned dorsoventrally and the anterior hyoid arch in an abnormal ventral position (Cobcroft, Pankhurst, Sadler & Hart 2001; Battaglene & Cobcroft 2007); gilthead seabream (*Sparus aurata*) with deformed lower jaw and undeveloped premaxilla (Fernández, Hontoria, Ortiz-Delgado, Kotzamanis, Estevez, Zambonino-Infante & Gisbert 2008) and barramundi (*Lates calcarifer*), with shortened and twisted jaws and a deformity named 'pinched jaw' which affects upper and/or lower jaws and gives the appearance of a pinched effect on the lateral surfaces of the jaw component (Fraser & de Nys 2005). Many abnormal jaw phenotypes have been previously described in yellowtail kingfish, such as elongated or reduced lower jaw, lower jaw bent down on one side, fusion of the jaw, twisted lower or upper jaw, and hyoid arch malformation characterized by a lowered hyoid arch with the hypohyal ventral to Meckel's cartilage (Cobcroft, Pankhurst, Poortenaar, Hickman & Tait 2004; Cobcroft & Battaglene 2013). The previous jaw abnormalities in *S. lalandi* were described between 23 and 45 dph (Cobcroft & Battaglene 2013), and the hyoid arch abnormality phenotype was described as early as 4 dph (Cobcroft *et al.* 2004). In comparison, jaw abnormalities described in striped trumpeter were detectable in flexion larvae at 10 mm total length (25 dph) (Battaglene & Cobcroft 2007), while in barramundi jaw deformations were not apparent until 18 dph (Fraser & de Nys 2005).

Descriptive studies of morphogenesis of jaw structures in early development are essential to identify the timing at which abnormalities arise and the specific skeletal components affected. Taking into account the high variability and unpredictability of jaw abnormalities among batches of eggs, early recognition and quantification of abnormal larvae would be useful for hatchery managers, to terminate early a culture with high prevalence of malformation, to reduce hatchery expenses of fish that would be culled later. Efforts in this regard are required to improve quality of cultured larvae and juveniles.

In this study, we present a characterization of abnormal phenotypes affecting cartilaginous elements of the jaw during the first 9 days of larval development in intense culture. Jaw shape variation is a fundamental feature but very challenging to quantify. To compare shape differences and distinguish abnormal from normal phenotypes, a landmark-based geometric analysis was performed to remove variation in size, rotation and position, thus allowing shape comparisons.

Materials and methods

Yellowtail kingfish larvae were obtained from wild fish (18 dams, 16 sires) captured in Taltal in the Province of Antofagasta and were reared at 21 °C at the hatchery of the Facultad de Ciencias del

Mar y Recursos Biológicos, Universidad de Antofagasta, Antofagasta, Chile. Natural reproduction is between November and March, corresponding to the spring–summer period of the Southern Hemisphere. The temperature of the water was maintained between 19 and 21 °C with a photoperiod of 16 h light and 8 h dark. Spawning occurred daily during the late afternoon. Fertilized eggs were collected 8–10 h after spawning, using a 500-μm net placed at the overflow pipe of the tank; the net was checked on a daily basis. Buoyant eggs were incubated in 45-L cylindrical tanks (500 eggs L^{-1}) at 21 °C with a constant sea water exchange of 2 L min^{-1} during the 48–60 h until hatching. Larval development time is given in days post hatching (dph) and total length (mm) (Sæle & Pittman 2010). Larvae were reared in 3000-L circular tanks at a density of 20 larvae L^{-1} in filtered (1 μm) and sterilized (UV light) sea water (35 psu) at 20 °C. At 3 dph (4.43 ± 0,03 mm), they were fed with *Brachionus plicatilis* enriched with Ori-Green (Skretting, Vervins, France) and AlgaMac 3050 (Bio-Marine, Hawthorne, CA, USA), added to each tank twice a day and adjusted to 2–4 rotifers mL^{-1}. *Nannochloropsis oculata* were added to larval rearing tanks at a density of 400 000 cells mL^{-1} throughout the period of feeding. *Artemia* nauplii enriched with Ori-Green (Skretting) were introduced in each rearing tank from 10 to 24 dph at 1–2 individuals mL^{-1}.

Samples of 70–150 larvae were collected during the summer period of 2013–2014 (November to January) from 3 cohorts at hatching (4.05 ± 0.05 mm total length), 2 dph (4.32 ± 0.10 mm), 3 dph (4.43 ± 0.03 mm), 4 dph (4.65 ± 0.15 mm), 6 dph (5.11 ± 0.12 mm) and 9 dph (5.66 ± 0.13 mm). Larvae were anaesthetized in 1% benzocaine and fixed overnight in 4% paraformaldehyde. Larvae were cleared in hydrogen peroxide solution and incubated overnight in 0.1% alcian blue for cartilage staining (Taylor & Van Dyke 1985).

Lateral (left side) and ventral views of all specimens were photographed using a digital camera LWS-Camera-M (MiniVID LW Scientific) and placed directly on an Olympus SZ40 stereoscopic microscope, using SCOPEPHOTO 2.0 software (Hangzhou Scopetek Optics Electronic Co., Hangzhou, China). Each stained larva was positioned as perfectly lateral as possible, using the overlap of paired anatomical structures as guide. The angle between Meckel's cartilage and quadrate cartilage was measured using SCOPEPHOTO software, constructing an arc from the anterior extreme of Meckel's cartilage to the posterior extreme of the quadrate cartilage.

The position and nomenclature used to describe cartilage components of the jaw and malformed phenotypes visually was based on prior descriptions of normal development in yellowtail kingfish, Japanese flounder (*Paralichthys olivaceus*) and zebrafish (*Danio rerio*) (Schilling, Piotrowski, Grandel, Brand, Heisenberg, Jiang, Beuchle, Hammerschmidt, Kane, Mullins, vanEeden, Kelsh, FurutaniSeiki, Granato, Haffter, Odenthal, Warga, Trowe & NussleinVolhard 1996; Suzuki, Srivastava & Kurokawa 2000; Cobcroft *et al.* 2004) (Fig. 1a,c). For morphometric analysis, the homologous landmarks were defined based on two criteria: (i) to provide a good representation of cartilaginous jaw shape and (ii) maximum variation (Bookstein 1991, 1997). Seven type II landmarks were used for the lateral view: (i) anterior

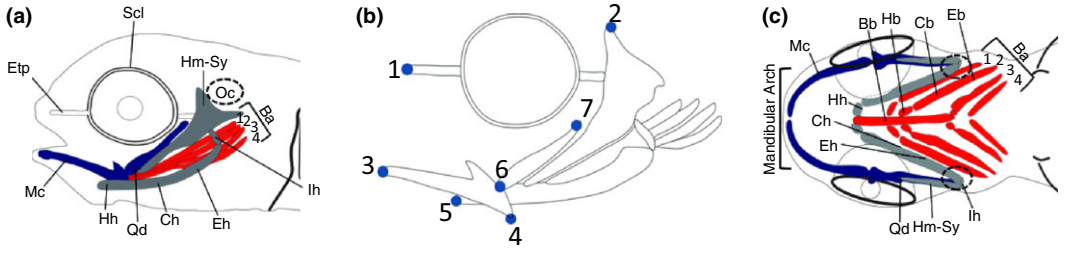

Figure 1 Diagram of cartilage structures and landmark map. Diagram of cartilage components of the jaw in lateral (a) and ventral (c) views and position of seven landmarks (b). Ba, Branchial arch; Bb, basibranchial cartilage; Cb, ceratobranchial cartilage; Ch, ceratohyal cartilage; Eb, epibranchial cartilage; Eh, epihyal cartilage; Hb, hypobranchial cartilage; Hh, hypohyal cartilage; Hm-Sy, hyosymplectic cartilage; Ih, interhyal cartilage; Mc, Meckel's cartilage; Oc, otic capsule; Qd, quadrate; Scl, sclerotic ring; Etp, ethmoid plate. [Colour figure can be viewed at wileyonlinelibrary.com]

tip of the ethmoid plate; (ii) dorso-anterior tip of hyomandibular-symplectic cartilage; (iii) anterior tip of Meckel's cartilage; (iv) posterior tip of Meckel's cartilage; (v) anterior tip of hypohyal cartilage; (vi) anterior tip of quadrate cartilage; and (vii) posterior tip of quadrate cartilage (Fig. 1b).

Landmark data were gathered using tps Util (Rohlf 2004) to construct the tps files and TPSdig2 (Rohlf 2005) to place the landmarks on the digital images. To remove all variation in size, rotation and position from the images, a generalized Procrustes analysis was performed (Rohlf & Slice 1990). This is currently the standard method for the analysis of landmark data and the most common geometric morphometric technique (Adams, Rohlf & Slice 2004). TpsRelw then performs relative warp analysis of shape variation relative to spatial scale (Bookstein 1989, 1991; Rohlf 2003). Finally, the software allows visualization of the variation in shape pattern by applying the thin-plate spline function. Images in the extreme values of each axis, relative warp scores and their corresponding eigenvalues were recorded for graph constructions (Rohlf 1990).

Results

Because craniofacial structures are bilaterally symmetrical, only a lateral view of the left side of the head is shown (Fig. 2). Cartilaginous structures became visible at 2 dph (4.27 mm TL) under weak alcian blue staining (Fig. 2a). The first pharyngeal arch or mandibular arch, formed by Meckel's and quadrate cartilage, is recognizable at 3 dph (4.40 mm TL) (Figs 1a and 2c). The paired Meckel's cartilages form the mandibular arch (Fig. 1c); each Meckel's cartilage forms an angle of 120° with the quadrate cartilage and together they form the suspensorium of the jaw (Fig. 1a). Cartilage associated with the neurocranium was visible at 3 dph (4.40 mm TL). The ethmoid plate extends anteriorly to the level of the anterior margin of the eyes and posteriorly to the anterior margin of the otic capsule (Figs 1a and 2c). The cartilaginous sclerotic was visible around the eye. The second and third pharyngeal arches were defined at 4 dph (4.6 mm TL) (Fig. 2e), coinciding with the onset of exogenous feeding. The second pharyngeal or hyoid arch is composed of hyomandibular-symplectic, hypohyal, ceratohyal and epihyal cartilages (Fig. 1a,c). The hyomandibular-symplectic is triangular in shape and oriented in the same angle as quadrate cartilage. The third pharyngeal arch is composed of four branchial arches formed by ceratobranchial and hypobranchial cartilages that converge ventrally at the basibranchial cartilage (Figs 1a,c and 2e). At 9 dph (5.6 mm TL), the cartilaginous epiphysial tectum, the supraorbital cartilages and the auditory capsules are developed (Fig. 2i).

At 4 dph (4.65 ± 0.15 mm TL), four different phenotypes were observed and classified according to the patterns and jaw shape components previously described (Fig. 2). In normal larvae (N), the hypohyal was just level with Meckel's cartilage (Fig. 2e). The first abnormal phenotype (M1) is characterized by an extension of Meckel's cartilage and was observed at 4, 6 and 9 dph (Fig. 2b and data not shown). The second abnormal phenotype (M2) was observed at 4 dph (4.60 mm TL), 6 dph (5.15 mm TL) and 9 dph (5.70 mm TL) (Fig. 2d,h, j). The ceratohyal and hypohyal cartilages are displaced ventrally and below Meckel's cartilage, and the quadrate is almost linear with Meckel's cartilage. The third abnormal phenotype (M3) was the least frequent abnormality and only observed at 4 dph (4.50 mm TL). It is characterized by shortening and dorsal flexion of the lower jaw (Fig. 2f).

The quantification of normal and abnormal phenotypes in three different cohorts was performed by visual assessment at 4 and 9 dph. We could not quantify 6 dph larvae because we did not have enough larvae from the three different cohorts. At 4 dph, 45%, 47% and 44% of all larvae were abnormal in cohorts 1, 2 and 3 respectively (Table 1). The M3 phenotype was observed only in some of the cohorts at 4 dph. Abnormal larval phenotypes characterized by twisting lower jaw laterally to one side, fusion of the jaw or by broken Meckel's cartilage were not found during the larval stages analysed.

Fifty-two 4 dph (4.62 ± 0.15 mm TL) larvae previously classified by visual assessment as normal (n = 22), M1 (n = 10) and M2 (n = 20) were analysed by relative warp analysis (Fig. 3). The M3 phenotype was not included because of the low number of individuals. A single specimen of 6 dph (5.13 mm TL) visually classified as M2 was included in this analysis. The first relative warp (horizontal axis) explained 48.77% of total shape variation and clearly separates phenotype M2 from normal (N) and M1 phenotypes. All M2 specimens were placed with positive values on the first warp including the 6 dph M2 larva; M1 specimens were placed either at zero or negative

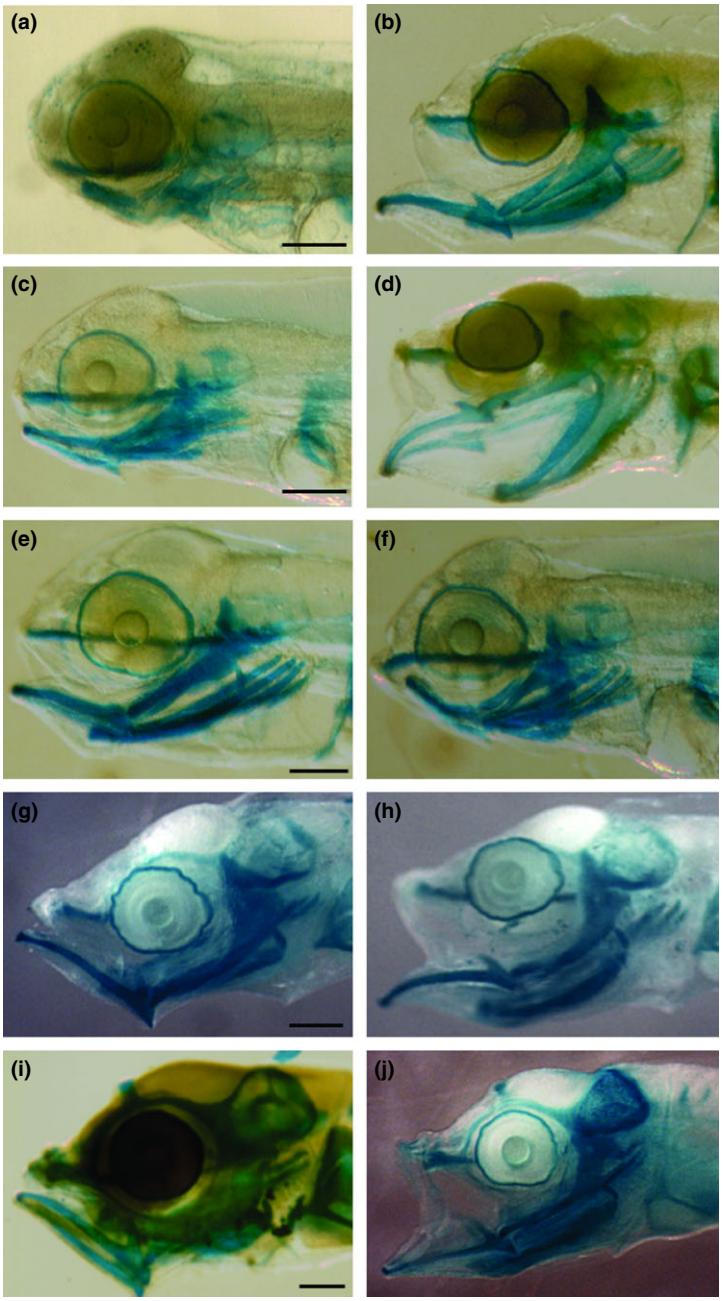

Figure 2 Lateral view of larval phenotypes (a) 2 dph (4.27 mm TL) normal larva, (b) 4 dph (4.68 mm TL) abnormal phenotype 1 (M1), (c) 3 dph (4.40 mm TL) normal larva, (d) 4 dph (4.60 mm TL) abnormal phenotype 2 (M2), (e) 4 dph (4.60 mm TL) normal larva, (f) 4 dph (4.50 mm TL) abnormal phenotype 3 (M3), (g) 6 dph (5.00 mm TL) normal larva, (h) 6 dph (5.15 mm TL) abnormal phenotype 2 (M2), (i) 9 dph (5.70 mm TL) normal larva and (j) 9 dph (5.60 mmTL) abnormal phenotype 2 (M2). Scale bar is 200 μm. [Colour figure can be viewed at wileyonlinelibrary.com]

values, while N specimens were centred in negative values although a few N specimens had positive values. Deformation grids along axis RW1 (Fig. 3d) revealed shape differences with respect to the consensus (Fig. 3b) and were associated with ventral displacement of ceratohyal and hypohyal cartilages (landmark 5). The second relative warp explained 19% of the variance and differentiated M1 from N phenotypes. All M1 phenotypes were placed on the negative side of the axis, whereas most N phenotypes were on the positive side. Deformation grids along this axis (Fig. 3c) also revealed shape differences with respect to the consensus (Fig. 3b) and were associated with elongated Meckel's cartilage.

Discussion

Craniofacial development in fish can be broadly divided into chronological stage processes related

Table 1 Percentage of normal (N), abnormal phenotype 1 (M1), abnormal phenotype 2 (M2) and abnormal phenotype 3 (M3) in three cohorts at 4 and 9 dph

			Jaw phenotype percentage				
Cohort	dph	T. length	N	M1	M2	M3	Total number of larval examined
1	4	4.79 ± 0.07	55	10	28	7	60
	9	5.67 ± 0.12	66	31	3	0	67
2	4	4.62 ± 0.15	53	41	4	2	113
	9	5.61 ± 0.10	52	30	18	0	44
3	4	4.60 ± 0.11	56	29	15	0	45
	9	5.62 ± 0.12	45	39	17	0	60

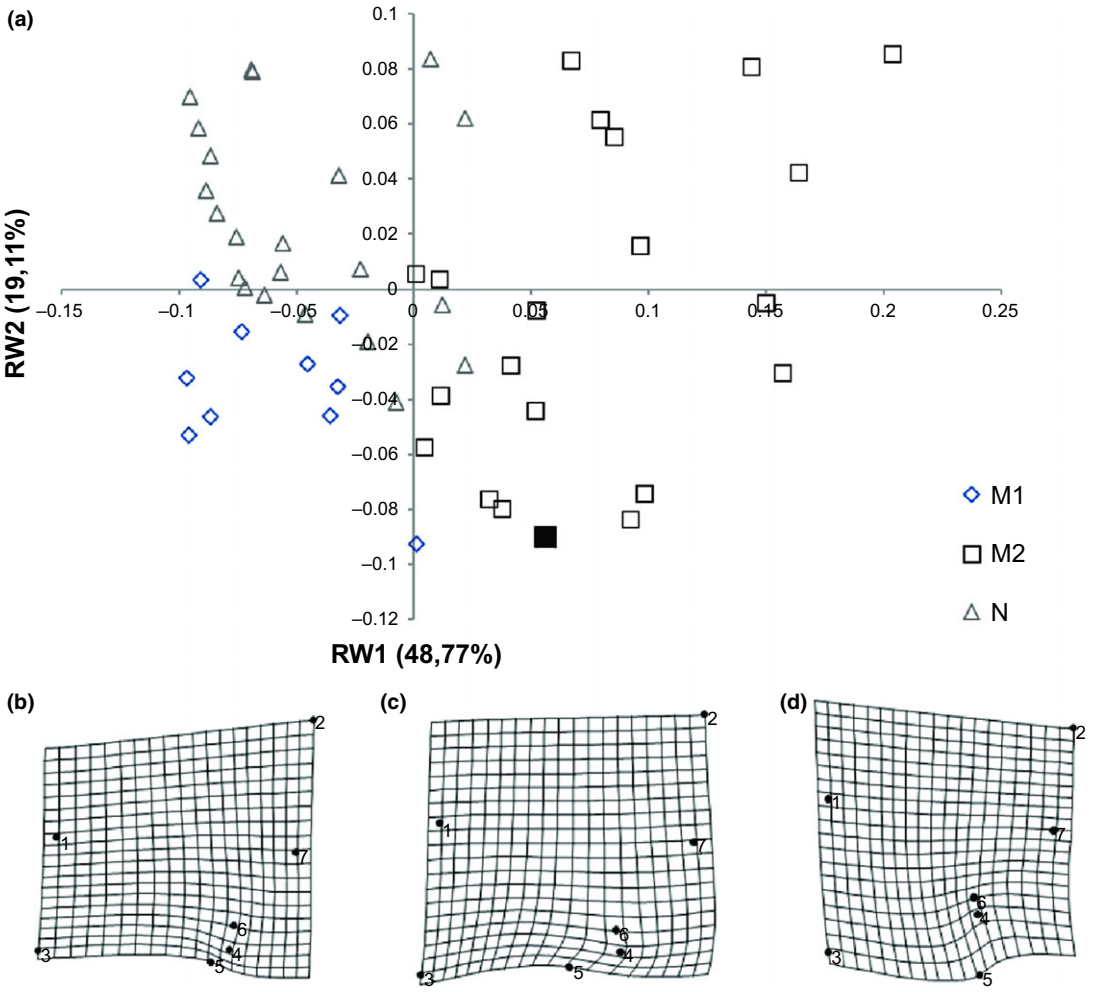

Figure 3 Results of a relative warp analysis on jaw shape of 52 4 dph (4.62 ± 0.15 mm TL) larvae previously classified as normal (N), M1 and M2. (a) Scatter plot of relative warp 1 versus relative warp 2 scores; (b) mean projection of normal phenotype; (c) mean projection of phenotypes M1 and (d) M2. Black square represents one 6 dph larva previously classified by visual assessment as M2. [Colour figure can be viewed at wileyonlinelibrary.com]

to: (i) cartilage development (during embryonic and early larval stages), (ii) bone development (larval stage), (iii) bone growth and (iv) bone remodelling, initiated during larval development and continuing through juvenile and adult stages (Parson, Andreeva, Cooper, Yelick & Albertson 2011). At early stages of embryonic development, a cell population termed cranial neural crest are induced,

migrate, condense and differentiate to form the craniofacial cartilages (Le Douarin & Dupin 2003). These cartilages thereafter develop into pharyngeal bones and other skull components by ossification of a cartilaginous precursor. However, the cranial dermal bones (frontal, infraorbitals, nasal, dentary, maxillary and opercula, among others) are formed in the mesenchyme or in the dermis by a different mechanism and without a cartilaginous template. All of the bone components are formed by the end of metamorphosis (Boglione, Gavaia, Koumoundouros, Gisbert, Moren, Fontagné & Witten 2013). Considering the complexity of cartilage and bone development, understanding the ontogeny of skeletal malformation in farmed fish and the potential contribution of external and internal factors requires consideration of the timing at which individual skeletal elements are formed.

According to the defined development stages of yellowtail kingfish (*S. lalandi*) by Martínez-Montaño, González-Álvarez, Lazo, Audelo-Naranjo and Vélez-Medel (2014), our results reveal that jaw cartilage components are completely formed by 4 dph (4.65 ± 0.05 mm) in yolksac–preflexion transition larvae. At 2 dph (4.32 ± 0.01 mm) and 3 dph (4.43 ± 0.03 mm), a weak and blurred alcian blue staining is observed showing that some cartilage are visible but not clearly defined. Therefore, we were not able to detect the presence of anomalies at this stage. At 4 dph (4.65 ± 0.05 mm), a high percentage of larvae have abnormal elongated Meckel's cartilage phenotype (M1 phenotype). Additionally, many larvae at 4 and 6 dph with the M2 phenotype also showed a ventral bending of the anterior tip of Meckel's cartilage (Fig. 2b,d,h) as has been previously described for yellowtail kingfish (Cobcroft *et al.* 2004; Cobcroft & Battaglene 2013). However, we did not quantify the extent of this bending. The observed hyoid arch abnormality characterized by ventral projection of ceratohyal and hypohyal cartilages (M2 phenotype) was similar to the phenotype reported by Cobcroft *et al.* (2004), at 4 and 9 days post hatching of yellowtail kingfish larvae and in early stage larvae of gilthead seabream (*S. aurata*) (Koumoundouros 2010) and striped trumpeter (*L. lineata*) (Battaglene & Cobcroft 2007). A similar lowered hyoid arch phenotype was reported for golden pompano (*Trachonotus ovatus*) at 5 and 16 dph (Ma, Zheng, Guo, Zhang, Jiang, Zhang & Qin 2014). The hyoid arch malformation phenotypes resemble the 'open mouth' phenotype found at juvenile stage, characterized by the incapacity to articulate the jaw. To follow this phenotype at later stages during bone development and growth would help to understand the evolution of this deformity. Jaw abnormalities described in yellowtail kingfish, that is lower jaw bending to one side or twisted and fusion of the jaw (Cobcroft & Battaglene 2013), were not observed at early larval stages during cartilage development, suggesting that these malformations originate at a later time and might be related to physical damage of normal cartilage structures or alterations during cartilage ossification or bone development. The M3 phenotype resembles lower jaw reduction deformity described for yellowtail kingfish; however, it was present in only a few individuals at 4 dph (4.79 ± 0.07 mm TL).

The finding that about 45% abnormal larvae are observed before first feeding suggests that both nutritional factors present in the embryonic yolk and broodstock rearing conditions and alimentation need to be studied as possible causative factors affecting patterning and differentiation of some cartilage components during larval development. However, the role of larval nutrition and egg and larval rearing conditions should not be ruled out, as nutritional imbalances and environmental parameters such as inadequate light, high water rate change, high stocking density, walling behaviour and temperature variation may either increase abnormalities or potentially generate new ones later during bone formation (Abdel, Abellan, Lopez-Albors, Valdes, Nortes & Garcia-Alcazar 2004; Georgakopoulou, Angelopoulou, Kaspiris, Divanach & Koumoundouros 2007; Cobcroft & Battaglene 2009, 2013; Boglione, Gisbert, Gavaia, Witten, Moren, Fontagné & Koumoundouros 2013).

In the hatchery, the larval survey performed revealed that after 30 days of culture between 30% and 40% from the total larvae reared after hatching remained alive, which is considered normal by yellowtail kingfish hatchery managers (R. Wilson, pers. comm.). The early appearance of abnormalities could be associated with the high mortality rate observed at the onset of larval feeding due to an inability to eat properly. However, a direct correlation between deformities and mortality has not been established and the most severe malformation are present at juvenile stages.

Geometric morphometrics has been used extensively to study shape changes in fish (Parson, Robinson & Hrbek 2003; Verhaegen, Adriaens, De Wolf, Dhert & Sorgeloos 2007). By defining seven

landmarks and using geometric morphometric analysis, we were able to describe phenotypes qualitatively in 4 dph larvae and classify them into three different groups: one related to normal phenotype (N) and two related to abnormal phenotype (M1 and M2). Overlap of some larvae previously classified by visual examination as N with M1 and M2 phenotypes revealed the existence of discrete differences in jaw morphology and suggest that visual classification may fail in to discriminate abnormal from normal specimens. Alternatively, those individuals who overlap would be showing the beginning of the deformity; however, further analysis with more specimens needs to be performed in order to support this statistically. The 6 dph larva included in the analysis was classified as M2 phenotype together with 4 dph M2 larvae, suggesting that individuals of a different size exhibit the same defective phenotype derived by morphometric analysis. Using the seven landmarks described in this study, it is possible to analyse jaw shape in larvae from 4 to 6 dph; however, to study the progression of abnormalities during flexion and post-flexion, larval development requires establishing new landmarks in cartilage and in bone structures throughout ossification. Our results show that this geometric morphometric analysis would also be a useful method for early recognition of anomalies affecting cartilaginous elements of the larval jaw.

Acknowledgements

This research was supported by Universidad de Antofagasta and Fondo de Inovación para la Competitividad, Gobierno Regional de Antofagasta. We thank Dr. John Gold for valuable comments to the manuscript.

Conflict of interest

All authors have no conflict of interest to declare.

References

Abdel I., Abellan E., Lopez-Albors O., Valdes P., Nortes M.J. & Garcia-Alcazar A. (2004) Abnormalities in the juvenile stage of sea bass (*Dicentrarchus labrax* L.) reared at different temperatures: types, prevalence and effect on growth. *Aquaculture International* **12**, 523–538.

Adams D.C., Rohlf F.J. & Slice D.E. (2004) Geometric morphometrics: ten years of progress following the "revolution". *Italian Journal of Zoology* **71**, 5–16.

Barahona-Fernandes M.H. (1982) Body deformation in hatchery reared European sea bass: *Dicentrarchus labrax* (L.). Types, prevalence and effect on fish survival. *Journal of Fish Biology* **21**, 239–249.

Battaglene S.C. & Cobcroft J.M. (2007) Advances in the culture of striped trumpeter larvae: a review. *Aquaculture* **268**, 195–208.

Boglione C., Gavaia P., Koumoundouros G., Gisbert E., Moren M., Fontagné S. & Witten P.E. (2013) Skeletal anomalies in reared European fish larvae and juveniles. Part 1: normal and anomalous skeletogenic processes. *Reviews in Aquaculture* **5**, S99–S120.

Boglione C., Gisbert E., Gavaia P., Witten P.E., Moren M., Fontagné S. & Koumoundouros G. (2013) Skeletal anomalies in reared European fish larvae and juveniles. Part 2: main typologies, occurrences and causative factors. *Reviews in Aquaculture* **5**, S121–S167.

Bookstein F.L. (1989) Principal warps: thin-plate splines and the decomposition of deformations. *Institute of Electrical and Electronics Engineers, Transactions on Pattern Analysis and Machine Intelligence* **11**, 567–585.

Bookstein F.L. (1991) *Morphometric Tools for Landmark Data: Geometry and Biology*. Cambridge University Press, Cambridge, UK.

Bookstein F.L. (1997) Landmark methods for forms without landmarks: morphometrics of group differences in outline shape. *Medical Image Analysis* **1**, 225–243.

Cloutier R., Lambrey de Souza J., Browman H.I. & Skiftesvik A.B. (2011) Early ontogeny of the Atlantic halibut *Hippoglossus hippoglossus* head. *Journal of Fish Biology* **78**, 1035–1053.

Cobcroft J.M. & Battaglene S.C. (2009) Jaw malformation in striped trumpeter *Latris lineata* larvae linked to walling behaviour and tank colour. *Aquaculture* **289**, 274–282.

Cobcroft J.M. & Battaglene S.C. (2013) Skeletal malformations in Australian marine finfish hatcheries. *Aquaculture* **396–399**, 51–58.

Cobcroft J.M., Pankhurst P.M., Sadler J. & Hart P.R. (2001) Jaw development and malformation in cultured striped trumpeter *Latris lineata*. *Aquaculture* **199**, 267–282.

Cobcroft J.M., Pankhurst P.M., Poortenaar C., Hickman B. & Tait M. (2004) Jaw malformation in cultured yellowtail kingfish (*Seriola lalandi*) larvae. *New Zealand Journal of Marine and Freshwater Research* **38**, 67–71.

Daoulas Ch., Economou A.N. & Bantavas I. (1991) Osteological abnormalities in laboratory reared sea-bass (*Dicentrarchus labrax*) fingerlings. *Aquaculture* **97**, 169–180.

Fernández I., Hontoria F., Ortiz-Delgado J.B., Kotzamanis Y., Estevez A., Zambonino-Infante J.L. & Gisbert E. (2008) Larval performance and skeletal deformities in farmed gilthead sea bream (*Sparus aurata*) fed with graded levels of Vitamin A enriched rotifers (*Brachionus plicatilis*). *Aquaculture* **283**, 102–115.

Fernández G., Cichero D., Patel A. & Martinez V. (2015) Genetic structure of Chilean populations of *Seriola*

lalandi for the diversification of the national aquaculture in the north of Chile. *Latin American Journal of Aquatic Research* **43**, 374–379.

Fraser M.R. & de Nys R. (2005) The morphology and occurrence of jaw and operculum deformities in cultured barramundi (*Lates calcarifer*) larvae. *Aquaculture* **250**, 496–503.

Georgakopoulou E., Angelopoulou A., Kaspiris P., Divanach P. & Koumoundouros G. (2007) Temperature effects on cranial deformities in European sea bass, *Dicentrarchus labrax* (L.). *Journal of Applied Ichthyology* **23**, 99–103.

Ibieta P., Tapia V., Venegas C., Hausdorf M. & Takle H. (2011) *Chilean Salmon Farming on the Horizon of Sustainability: Review of the Development of a Highly Intensive Production, the ISA Crisis and Implemented Actions to Reconstruct a More Sustainable Aquaculture Industry, Aquaculture and the Environment – A Shared Destiny*, (ed. by B. Sladonja), pp. 251–246. INTECH Open Acces Publisher.

Koumoundouros G. (2010) Morpho-anatomical abnormalities in mediterranean marine aquaculture. *Recent Advances in Aquaculture Research* **66**, 125–148.

Le Douarin N.M. & Dupin E. (2003) Multipotentiality of the neural crest. *Current Opinion in Genetics and Development* **13**, 529–536.

Lewis L.M. & Lall S.P. (2006) Development of the axial skeleton and skeletal abnormalities of Atlantic halibut (*Hippoglossus hippoglossus*) from first feeding through metamorphosis. *Aquaculture* **257**, 124–135.

Ma Z., Zheng P., Guo H., Zhang N., Jiang S., Zhang D. & Qin J.G. (2014) Jaw malformation of hatchery reared golden pompano *Trachinotus ovatus* (Linnaeus 1758) larvae. *Aquaculture Research* **47**, 1141–1149.

Martínez-Montaño E., González-Álvarez K., Lazo J.P., Audelo-Naranjo J.M. & Vélez-Medel A. (2014) Morphological development and allometric growth of yellowtail kingfish *Seriola lalandi V*. larvae under culture conditions. *Aquaculture Research* **47**, 1277–1287.

Matsuoka M. (2003) Comparison of meristic variations and bone abnormalities between wild and laboratory-reared Red Sea Bream. *Japan Agricultural Research Quarterly* **37**, 21–30.

Moran D., Smith C.K., Gara B. & Poortenaar C.W. (2007) Reproductive behaviour and early development in yellowtail kingfish (*Seriola lalandi* Valenciennes 1833). *Aquaculture* **262**, 95–104.

Moran D., Pether S.J. & Lee P.S. (2009) Growth, feed conversion and faecal discharge of yellowtail kingfish (*Seriola lalandi*) fed three commercial diets. *New Zealand Journal of Marine and Freshwater Research* **43**, 917–927.

Parson K.J., Robinson B.W. & Hrbek T. (2003) Getting into shape: an empirical comparison of traditional truss-based morphometric methods with a newer geometric method applied to new world cichilds. *Environmental Biology of Fishes* **67**, 417–431.

Parson K.J., Andreeva V., Cooper W.J., Yelick P.C. & Albertson R.C. (2011) Morphogenesis of the zebrafish jaw: development beyond the embryo. *Methods in Cell Biology* **101**, 225–248.

Poortenaar C.W., Hooker S.H. & Sharp N. (2001) Assessment of yellowtail kingfish (*Seriola lalandi lalandi*) reproductive physiology, as a basis for aquaculture development. *Aquaculture* **201**, 271–286.

Rohlf F.J. (1990) Morphometrics. *Annual Reviews of Ecology and Systematics* **21**, 299–316.

Rohlf F.J. (2003) tpsRelw, relative warps analysis, version 1.36. Department of Ecology and Evolution, State University of New York, Stony Brook, NY, USA.

Rohlf F.J. (2004) tpsUtil: Thin Plate Spline Utility (Version 1.33). State University of New York at Stony Brook, Stony Brook, NY, USA.

Rohlf F.J. (2005) tpsDig, digitize landmarks and outlines, version 2.05. Department of Ecology and Evolution, State University of New York, Stony Brook, NY, USA.

Rohlf F.J. & Slice D.E. (1990) Extensions of the Procrustes method for the optimal superimposition of landmarks. *Systematic Zoology* **39**, 40–59.

Sæle Ø. & Pittman K. (2010) Looking closer at the determining of a phenotype? Compare by stages or size, not age. *Journal of Applied Ichthyology* **26**, 294–297.

Schilling T.F., Piotrowski T., Grandel H., Brand M., Heisenberg C.P., Jiang Y.J., Beuchle D., Hammerschmidt M., Kane D.A., Mullins M.C., vanEeden F.J.M., Kelsh R.N., FurutaniSeiki M., Granato M., Haffter P., Odenthal J., Warga R.M., Trowe T. & NusslеinVolhard C. (1996) Jaw and branchial arch mutants in zebrafish. 1. Branchial arches. *Development* **123**, 329–344.

Suzuki T., Srivastava A.S. & Kurokawa T. (2000) Experimental induction of jaw, gill and pectoral fin malformations in Japanese flounder, *Paralichthys olivaceus*, larvae. *Aquaculture* **185**, 175–187.

Taylor W.R. & Van Dyke G.C. (1985) Revised procedures for staining and clearing small fishes and other vertebrates for bone and cartilage study. *Revue Internationale d'Ichtyologie* **9**, 107–119.

Verhaegen Y., Adriaens D., De Wolf T., Dhert P. & Sorgeloos P. (2007) Deformities in larval gilthead sea bream (*Sparus aurata*): a qualitative and quantitative analysis using geometric morphometrics. *Aquaculture* **268**, 156–168.

Wilson R., Ramos R., Abarca M. & Plaza J. (2012) Optimización de una Tecnología para la Producción de Juveniles de "dorado" (*Seriola lalandi*) como Unidad Base para Proyectar la Sustentación del Proceso de Engorda a Escala Comercial. Final Project Report Corfo 07CT9 PDT-59. 98p.

